Microb Ecol (2016) 71:887–900
DOI 10.1007/s00248-016-0732-x

ENVIRONMENTAL MICROBIOLOGY

Annual Cycles of Two Cyanobacterial Mat Communities in Hydro-Terrestrial Habitats of the High Arctic

Daria Tashyreva[1,2] · **Josef Elster**[1,3]

Received: 12 August 2015 / Accepted: 18 January 2016 / Published online: 3 February 2016

Abstract Cyanobacteria form extensive macroscopic mats in shallow freshwater environments in the High Arctic and Antarctic. In these habitats, the communities are exposed to seasonal freezing and desiccation as well as to freeze–thawing and drying–rewetting cycles. Here, we characterized the annual cycles of two *Phormidium* communities in very shallow seepages located in central Svalbard. We observed the structure of the communities and the morphology, ultrastructure, metabolic activity, and viability of filaments and single cells. The communities overwintered as frozen mats, which were formed by long filaments enclosed in thick multilayered polysaccharide sheaths. No morphologically and/or ultrastructurally distinct spore-like cells were produced for surviving the winter, and the winter survival of the communities was not provided by a few resistant cells, which did not undergo visible morphological and ultrastructural transformations. Instead, a high proportion of cells in samples (85 %) remained viable after prolonged freezing. The sheaths were the only morphological adaption, which seemed to protect the trichomes from damage due to freezing and freeze-associated dehydration. The cells in the overwintering communities were not dormant, as all viable cells rapidly resumed respiration after thawing, and their nucleoids were not condensed. During the whole vegetative season, defined by the presence of water in a liquid state, the communities were constantly metabolically active and contained <1 % of dead and injured cells. The morphology and ultrastructure of the cells remained unaltered during observations throughout the year, except for light-induced changes in thylakoids. The dissemination events are likely to occur in spring as most of the trichomes were split into short fragments (hormogonia), a substantial proportion of which were released into the environment by gliding out of their sheaths, as well as by cracking and dissolving their sheaths. The short fragments subsequently grew longer and gradually produced new polysaccharide sheaths.

Keywords *Phormidium* · Life cycle · Overwintering · Polar Regions · Viability · Hormogonia

✉ Daria Tashyreva
tashyreva@butbn.cas.cz

[1] Centre for Polar Ecology, Faculty of Science, University of South Bohemia, České Budějovice, Czech Republic

[2] Botany Department, Faculty of Science, University of South Bohemia, České Budějovice, Czech Republic

[3] Institute of Botany, Academy of Sciences of the Czech Republic, Třeboň, Czech Republic

Introduction

Cyanobacteria are amongst the most abundant photosynthetic organisms in both the High Arctic and Antarctica, where they have to cope with harsh physical conditions and experience physiological stresses during much of the year [1, 2]. Despite these constraints, different taxa of cyanobacteria colonize a wide range of terrestrial and freshwater habitats including deep and shallow lakes, streams, glaciers, soils, and surfaces of rocks and may achieve considerable biomass in these environments [3].

Polar habitats are highly variable, with seasonal and diurnal fluctuations of environmental conditions such as temperature, light intensity, and availability of water and mineral nutrients [2–6]. The amount of water and its availability during the year greatly define the physicochemical stability of a particular

habitat and may affect the species composition and survival strategies of cyanobacteria. For instance, the presence of liquid water during the whole year in stable lacustrine environments enables organisms to avoid both freezing and desiccation [7, 8] as well as seasonal fluctuation of salinity related with freezing and drying [9]. Furthermore, due to its high heat capacity, water plays a role in maintaining a constant temperature regime [2]. In contrast, terrestrial habitats (e.g., fellfield soils) are characterized by great diurnal fluctuations of temperature, rapid and frequent drying–rewetting and freeze–thawing events, and long-term freezing and desiccation periods due to the limited availability of moisture [6].

In the present study, we focused attention on hydro-terrestrial habitats, in which water is available during spring melt and in early summer, but these often dry out by the end of summer and are completely frozen during winter [9]. Because most of these habitats are not shadowed, organisms there are exposed to continuous sunlight in summer months, which may exceed 2000 μmol m^{-2} s^{-2} on sunny days [10] and elevated levels of UV radiation [3], but they are devoid of light during polar winters. Furthermore, these environments are also subjected to drying–rewetting and repeated freeze–thawing episodes [4, 11]. In the Polar Regions, hydro-terrestrial habitats are commonly represented by shallow meltwater pools, streams, and seepages.

Species of *Phormidium*, a genus of filamentous cyanobacteria, are very common and often dominant in these habitats, where they form extensive macroscopic films and mats [12–16]. Despite the evidence that *Phormidium* species are well adapted to stresses occurring in hydro-terrestrial habitats [5, 11, 17], annual development of communities has not been described yet, and only a few studies have mentioned their overwintering strategy. The previous field studies employed community-level methods for assessing viability and physiological activity (e.g., measurement of respiration and photosynthesis measured by oxygen evolution/uptake, recovery of photosynthesis, etc.), but omitted observation of cell morphology and ultrastructure, and evaluation of viability and metabolic activity at the single-cell level [5, 18, 19]. Therefore, it is not known whether *Phormidium* species produce any structurally specialized cells to survive winter, their survival is attributed to only a few morphologically non-specialized cells, or their entire communities overwinter in a vegetative state.

This study describes a set of observations over the full annual cycle of two *Phormidium* communities in close vicinity of the CzechPolar station in the High Arctic (Petuniabukta, Billefjorden, Central Spitsbergen, Svalbard Archipelago). The description is based on field observation of populations in winter and from early summer to autumn, as well as on a spring thaw simulated under laboratory conditions. Both populations were represented by films/mats, one in a shallow meltwater stream and the other one in a shallow pool. During our study, we monitored the environmental conditions, described the spatial structure of the communities and the morphology and ultrastructure of cells and filaments, and assessed their viability and metabolic activity at the single-cell level. We aimed to investigate (i) whether viability, morphology, and ultrastructure of cells and filaments change during the vegetative season; (ii) the length of physiologically active period over the annual cycle; (iii) the overwintering strategy of the communities, including the proportion of cells which survive winter and their metabolic activity, morphology, and ultrastructure.

Materials and Methods

Study Site

The study site is located in the central part of Svalbard in the northernmost part of the Billefjorden, in Petunia bay (latitude 78° 40′ 49.3″ N; longitude 16° 27′ 18.1″ E), in close vicinity to the Josef Svoboda Czech Arctic Station. Vegetative seasons, defined by the availability of liquid water, in this area are relatively short. Recent 2-year measurements of meteorological parameters showed that mean ground surface temperature in this area exceeded 0 °C for about 4 months—from the end of May until the end of September. Snow cover, accordingly, persisted for approximately 8 months—from the beginning of October to the beginning of June (measured by the surface albedo). Relative air humidity fluctuated between 60 and 100 % except for a few drier episodes during winter [10].

The area is represented by an ice-free marine terrace with mainly mineral substrate covered with scarce moss vegetation. The substrate is saturated with water supplied mostly by melting of the permafrost, which forms numerous shallow (a few centimeters deep) pools and streams or seepages. These shallow water habitats often dry up by the end of summer.

Field Observations

We monitored two cyanobacterial seepage communities: a film from a slow-flowing shallow stream and a mat-like community from a shallow pool. Inside each of the sites, ten marked poles were installed for observation and repeated sampling. The biomass was sampled from those points and immediately used for viability assays. In addition, an aliquot of biomass from every point was fixed with 2 % p-formaldehyde for further laboratory light and electron microscopy investigation. The communities were sampled and photographed every 3 days during the observation periods. Observations of morphology and ultrastructure of cells and filaments were carried in both 2010 and 2011, but viability tests were carried out in 2011 only. The field observations included several periods: June 26 to July 15, 2010, and July

3 to 20, 2011 (late spring–early summer), and August 24 to September 15, 2010, and September 10 to 25, 2011 (late summer–autumn). Additionally, samples of frozen biomass from the sites were collected in the first half of April 2012 (winter samples), transported frozen at −15 °C to the Czech Republic and kept in a freezer at −15 to −20 °C. Since it was impossible to access the sites during spring melt, it was simulated under laboratory conditions using these samples.

In order to give a general thermal characteristic of habitats, the temperature in the study sites was measured with a Minikin T datalogger (EMS Brno, Czech Republic) at a 1-h interval. Minikin is a small datalogger with embedded sensors for precise monitoring of temperature with ±0.2 °C accuracy of probe. One datalogger was installed in the stream and the two others in a shallow and in the deeper part of the pool. The measurements were made between April 10, 2012, and August 18, 2012; temperature measurement in the deeper part of the pool continued until August 29, 2013. Due to technical reasons, temperature measurements during 2010–2011 were not possible. Incident global solar radiation was monitored with a LI-200 pyranometer (LI-COR, USA) at an automatic weather station (AWS) located about 3 km northwest of the study site. The AWS was located on a flat marine terrace at the geographical coordinates 78° 42.11′ N, 16° 27.64′ E and the altitude of 15 m a.s.l. (Láska et al. 2012). Radiation readings were recorded as 30-min averages.

Chemical Analysis of Water

Water was collected three times for chemical analysis (July 15, August 3, and September 20, 2011) from each of the sampling sites, filtered through GF/C filters (Whatman), transported to the Czech Republic, and stored frozen until the analysis.

Phosphorus (as dissolved reactive phosphorus (DRP)) and nitrogen (as dissolved inorganic nitrogen (DIN)) were determined spectrophotometrically using a flow injection analyzer (FIA, Lachat QC8500, USA). DRP (PO_4^{2-}-P) was analyzed by a reaction with ammonium molybdate and a reduction by stannous chloride to phosphomolybdenum blue (ISO 15681-1:2003). The detection limit for DRP was 10 μg l^{-1}. Nitrate nitrogen (NO_3^--N) was reduced to nitrite nitrogen (NO_2^--N) in cadmium column and analyzed by a reaction with sulfonamide and a subsequent reaction with N-(1-naphthyl)-ethylenediamine dihydrochloride (EN ISO 13395:1996). Ammonium nitrogen (NH_4^+-N) was measured by the gas diffusion method and a reaction with hydrogen iodide (EN ISO 11732). The detection limit for NH_4^+-N, NO_3^--N, and NO_2^--N was 10 μg l^{-1}. The sum of nitrate, nitrite, and ammonium nitrogen gave values of DIN. The total nitrogen (TN) and total phosphorus (TP) were measured as a concentration of NO_3^--N and PO_4^{2-}-P after mineralization with potassium persulfate (ISO 11905-1).

Laboratory Simulation of Spring Thaw

The frozen winter samples (including biomass and ice) were melted in Petri dishes at +4 °C and 150 μmol m^{-2} s^{-1} of white light, mixed with water collected from sampling sites during July, and incubated for 15 days. The appearance of the biomass and morphology of cells/filaments were observed immediately after melting and in 1, 2, 3, 7, and 15 days thereafter. Viability tests were carried out immediately after melting the biomass.

Viability Tests

Viability tests were based on simultaneous staining with three fluorescent dyes: 5-cyano-2,3-ditolyl tetrazolium chloride (CTC) was used to detect respiration, injuries to plasma membranes were tracked with SYTOX Green, and the presence and shape of nucleoids were shown with 4′,6-diamidino-2-phenylindole (DAPI). Samples of biomass were transferred to Eppendorf tubes with water from the sampling sites and shaken to remove sand and then collected and split into small pieces with preparation needles. The samples were stained with 10-μM solution of SYTOX Green for 45 min, post-stained with 5-mM CTC for 30 min and with 5 μg ml^{-1} DAPI for 30 min, and immersed into freshwater. While stained, the samples were incubated in the dark at actual outdoor temperature or at +4 °C in the spring thaw simulation experiment. According to the staining results, the cells were identified as (i) active and intact: CTC- and DAPI-positive, SYTOX Green-negative; (ii) active and injured: CTC-, DAPI-, and SYTOX Green-positive; (iii) inactive and intact or dormant: CTC- and SYTOX Green-negative, DAPI-positive; (iv) dead: CTC-negative, SYTOX Green- and DAPI-positive, or all negative. The detailed protocol for CTC, SYTOX Green, and DAPI co-staining of field-collected samples and properties of the dyes are described in Tashyreva et al. [20]. At least 2500 cells were counted in each of the observations.

Light and Fluorescence Microscopy

An Olympus BX53 microscope equipped with an Olympus DP72 microscope digital camera was utilized for observing the morphology of the cells and filaments using a resolution of 1024 × 1360 pixels. The optical system for fluorescence microscopy consisted of a 100-W ultrahigh-pressure mercury arc lamp and four filter cubes for separately observing each dye fluorescence (exCitation/emission/dichroic mirror): U-FUN filter cube for DAPI (360–370/460–510/420 nm), U-FBWA cube for SYTOX Green (460–495/510–550/505 nm), and combined filter cubes for CTC–formazan (425–445/570–625/455 nm) and autofluorescence of pigments (565–585 nm/600IF/595 nm). A series of several dark-field images

were acquired to record the fluorescence of each of the signals, and a bright-field image was taken for the total cell counts and morphology observation.

Transmission Electron Microscopy

In order to remove sand particles from the samples, an aliquot of cyanobacterial biomass was split into small pieces, re-suspended by shaking in 2 ml of distilled water, and collected with a micropipette. The cells were concentrated with mild centrifugation. Two parts of dense sand-free cell suspension were mixed with one part of 20 % bovine serum albumin cryoprotectant in a 0.1 M phosphate buffer. Three microliters of the mixture was placed into a flat specimen carrier made of gold-plated copper (height 0.5 mm; inner diameter 1.2 mm; depth 0.2 mm). The samples were rapidly frozen with liquid nitrogen under 2100-bar pressure using a Leica EM PACT2 high-pressure freezing machine. The frozen samples were quickly warmed up to −90 °C and freeze-substituted with 2 % OsO_4 in pure acetone for 96 h using Leica AFS system. Following that procedure, the samples were slowly warmed at +5 °C/h to −20 °C and subsequently at 3 °C/h to +3 °C. This was followed by 8 h at +3 °C and 18 h at +4 °C. The specimens were rinsed three times with anhydrous acetone and infiltrated in a mixture of acetone: Epon resin (2:1, 1:1, and 1:2 for 1 h at each step at room temperature). After overnight incubation in pure Epon, the material was released from the carriers, and the whole specimens were embedded in fresh resin and polymerized at +62 °C for 48 h. Ultrathin sections (70 nm) were cut using an ultramicrotome (UCT, Leica Microsystems, Vienna, Austria) and collected on formvar-coated copper grids. The grids were contrasted in ethanolic uranyl acetate and lead citrate and observed at 80 kV using a JEOL JEM 1010 transmission electron microscope equipped with MegaView III digital camera (SIS GmbH).

Results

Environmental Conditions

According to the measurements provided by the data loggers, the temperature reached zero in late May in both years and remained there while the snow and ice melted (Fig. 1a). Freezing began in the deeper part of pool at the end of September, after which the temperature fluctuated between

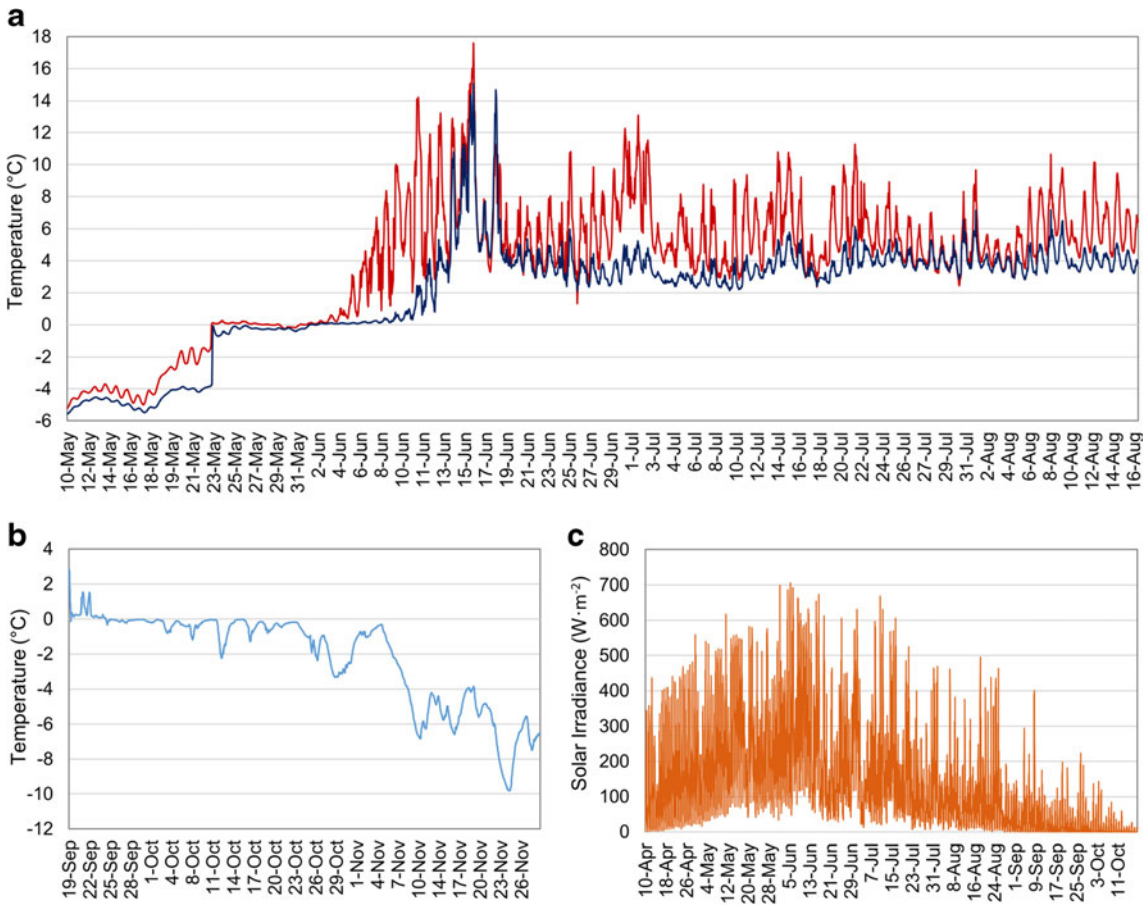

Fig. 1 Temperature in the deep part of the pool (*red chart*) and in the stream (*blue chart*) during spring and summer (**a**), temperature in the deeper part of pool during autumn (**b**), and solar irradiance in April–September (**c**), all in 2012

0.1 and −2.3 °C before the water became constantly frozen in late October (Fig. 1b). The minimum temperatures for both sampling sites were −11.1 and −11.4 °C. The highest temperatures were observed during the second half of June (2012): 15.3 °C in the deeper part of pool (Fig. 1a) and 14.8 °C in its shallow part (not shown) and 17.6 °C in the stream (Fig. 1a). The pool in its deeper part was more thermally stable with a smaller diurnal temperature fluctuation and notably colder than the stream and shallow part of the pool during the summer months (after snowmelt). The summer average/means of diurnal amplitudes were 4.0/2.3 °C in deeper part of the pool and 5.9/4.2 °C in its shallow part and 5.9 °C/5.2 °C in the stream. The annual temperature regime was as follows: gradual rising temperatures during snowmelt (the end of May), strong diurnal fluctuations till the second half of June, and weak diurnal fluctuations till late September, freeze–melt episodes at the end of vegetative season (in September–early October), and normally constantly subzero temperatures in winter (until spring snowmelt). However, 2 months before we collected the winter samples, there was an uncommon 2-week winter thaw in January–February 2012.

Changes of Water Chemistry During Season

Chemical analysis showed that concentrations of TN and phosphorus in the interconnected pool and stream were similar and did not change significantly during the observation, and there was no clear trend in change of total N/P ratio. Phosphate and nitrite concentrations were always below the detection limit of the method. The DIN content was slightly higher at the end of vegetative season, and the conductivity increased by a factor of 3.6 from July to the late September (Table 1).

Species Composition

Both communities were dominated by species identified according to their morphological and ultrastructural properties as *Phormidium* sp. Group VIII [21], which were morphologically identical but had a different shape of their nucleoids, when stained with DAPI (Fig. 2d, i). A group of *Phormidium* species has been recently transferred to the genus *Microcoleus* [22, 23]. However, both species belonged to the genus *Phormidium* according to cytomorphological criteria: cells are shorter (4 to 6 μm) than wide (8 to 9 μm); polar ends in trichomes are not narrowed and lack calyptra and apical cells are rounded; sheaths are multilayered and contain only one trichome (Fig. 3); thylakoids appear irregular in lengthwise section and are not arranged radially at cross sections (Fig. 4e); cell division is initiated before daughter cells from previous division grow to the size of the mother cell [24, 25; Komárek, personal communication].

Seasonal Changes of the Habitats and Communities

The sampling sites appeared similarly both years during first half of July: the depth of water in the pool was 2 to 7 cm, and the stream was shallower (<2 cm deep) so that cyanobacterial biomass was covered with only a thin layer of slowly running water. Both years, the sites were much drier in late summer and autumn (end of August and September) than in July. On the 24th of August 2010, both habitats were completely out of water, but the substrate underneath the communities was still wet. Nearly, the entire biomass from the pool community was wet, whereas the stream community was drier, and some parts of the crust were detached from the substrate and appeared to be completely dry. During the following month, the crusts were dried and rewetted several times with air moisture and occasional precipitation. On the 15th of September, the water and biomass in both sites were frozen solid but melt on the next day. In 2011, both communities were moist until the second half of September, and at least a small amount of water was available at any time of observation.

In late June and early July, both communities contained distinctly different pink and red areas (Fig. 5a). The pink biomass formed a tight crust, which was attached to the mineral substrate. The crust consisted mainly of empty extracellular polysaccharide (EPS) sheaths and relatively few trichomes enclosed in thick multilayered EPS sheaths, without inclusions or with big oil-like inclusions located at the cell centers (Fig. 3c, d). The color of pink biomass ranged from dark pink to white depending on the content of red, carotenoid-containing trichomes. Red biomass had a soft "cloudy" consistence and floated on the surface of water. The red biomass contained only long sheathless trichomes; many of the cells accumulated storage material, apparently cyanophycin and liquid oil-like inclusions of unknown nature, which were deposited mostly at the cross walls (Fig. 3a, b).

Table 1 Average for the pool and stream physicochemical properties of the water (means ± SD; $n = 6$)

Sample	Conductivity (μS cm^{-1})	N-NH_4 (μg l^{-1})	N-NO_2 (μg l^{-1})	N-NO_3 (μg l^{-1})	TN (μg l^{-1})	P-PO_4 (μg l^{-1})	TP (μg l^{-1})
July	176 ± 35.5	38 ± 18.8	<10	190.3 ± 46.7	362.7 ± 56.3	<10	19.3 ± 2.2
August	213.3 ± 39.4	21.8 ± 3.9	<10	140.2 ± 37.7	327.6 ± 114.6	<10	20.9 ± 4.9
September	635 ± 68.5	34.9 ± 8	<10	268.4 ± 44.9	414.5 ± 53.2	<10	23.2 ± 1.9

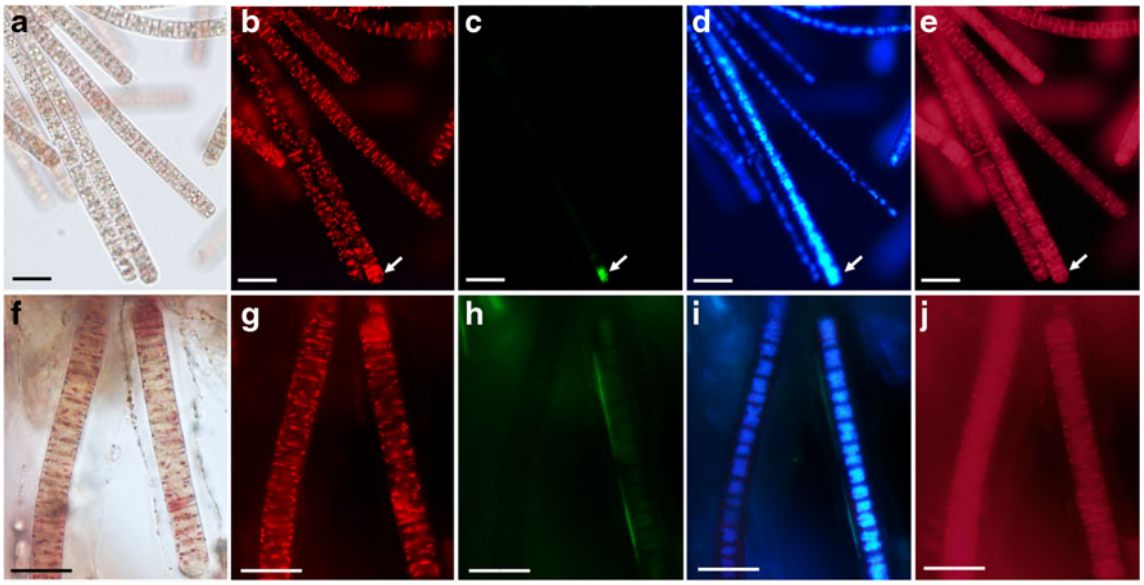

Fig. 2 Red biomass from the pool community (**a**–**e**) and pink biomass from the stream community (**f**–**j**) in the early summer, viewed by light microscopy (**a**, **f**) and stained with CTC (**b**, **g**), SYTOX Green (**c**, **h**), and DAPI (**d**, **i**) and showing weak pigment autofluorescence (**e**, **j**). The injured cell is marked with an *arrow*. *Scale bars* are 20 μm

Both years, in late summer–autumn (end of August and September), the communities appeared as continuous tight crusts with distinct red and pale pink areas (Fig. 5b). At the end of August, the biomass from the red areas of crusts was formed by long interlaced filaments, all enclosed in sheaths, with sand incorporated between them (Fig. 6a). In September, the sheaths became thick and often multilayered (Fig. 6b, d). A small number of trichomes disintegrated into short fragments or hormogonia. The pink biomass appeared similar as in July and consisted mainly of empty sheaths and a few filaments enclosed in thick multilayered sheaths. Some filaments in both red and pink areas of the crusts had big- or medium-size oil-like inclusions, whereas others lacked them completely. Cells from the pool community usually accumulated more material than cells from the stream community; in 2010, both sites contained more cells with inclusions than in 2011. Apart from presence of sheaths and inclusions, cells in both pink and red areas of each community were morphologically identical and did not change their morphology during vegetative season.

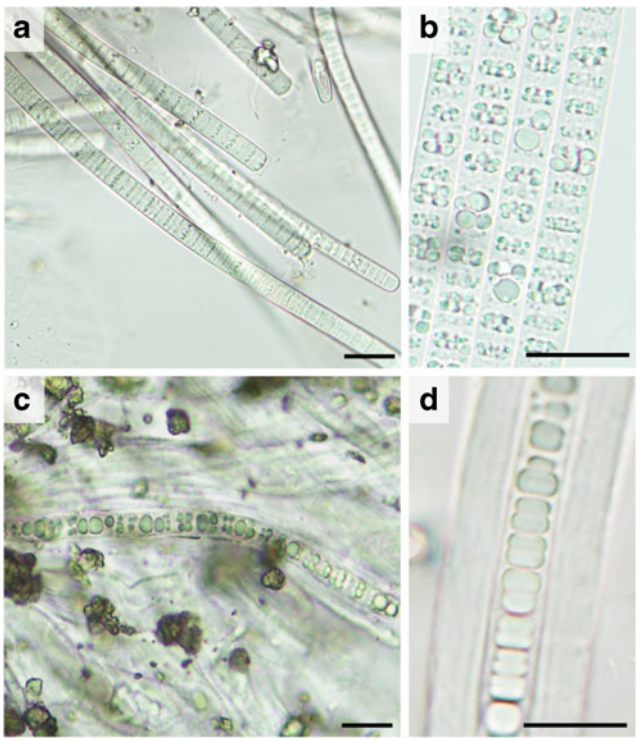

Fig. 3 Morphology of filaments in the early summer from red biomass (**a**, **b**) and pink biomass (**c**, **d**). Biomass is fixed with formaldehyde. *Scale bars* are 20 μm

Ultrastructure of Cells

Samples collected from the red areas of both studied sites were examined by electron microscopy. Preparation of samples from the pink areas as well as a sample of crust, collected in winter from the pool, was not possible since the samples contained numerous non-removable sand particles bound to EPS sheaths.

Early Summer Samples

Electron microscopy showed that the central cytoplasm of cells contained dispersed, unfolded nucleoids and numerous polyhedral bodies (Fig. 4a, b). Nucleoplasm was surrounded by a peripheral system of a few solitary thylakoids of irregular pattern (Fig. 4a, b). The thylakoid membranes were often

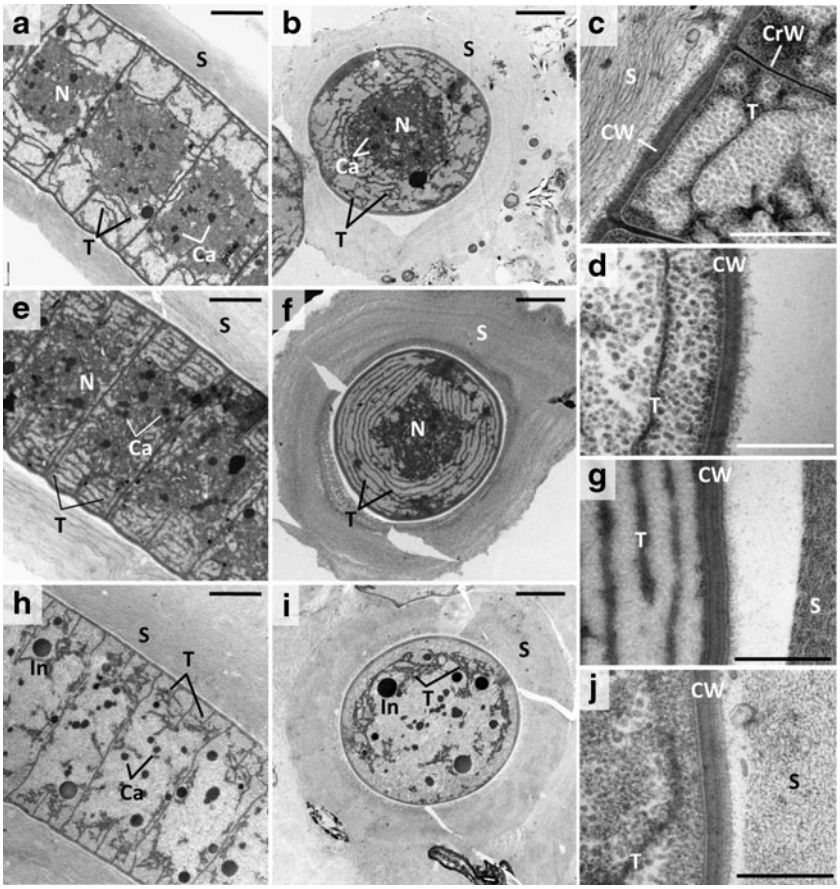

Fig. 4 Ultrastructure of cells and filaments of red biomass from the stream community. Longitude sections of filaments in the early summer (**a**), in autumn (**e**), and in winter (**h**); cross sections of cells in the early summer (**b**), in autumn (**f**), and in winter (**i**); longitude section of a cell with inhomogeneous cell wall in summer (**c**); cross sections through cell walls in the early summer (**d**), in autumn (**g**), and in winter (**j**). *Ca* carboxysomes, *CrW* cross walls, *CW* cell walls, *In* inclusions, *N* nucleoids, *S* EPS sheaths, *T* thylakoids. *Scale bars* are 2 μm and 500 nm (**c**, **d**, **g**, **j**)

separated with a wide space or formed large sac-like vesicles (Fig. 4b). There were no discernable phycobilisomes on the outer surface of thylakoid membranes with the maximum magnification of 100,000, which we employed. The cell envelopes had structure, typical for Oscillatoriaceae [26]: a thick peptidoglycan layer deposited between an outer cell membrane and plasmalemma and an external serrated layer (Fig. 4c). Formation of new cross walls preceded formation of a continuous cell wall from previous cell division (Fig. 4a). The thickness of the cell walls in cross sections ranged from 61 to 74 nm. However, the longitude sections revealed that cell walls were inhomogeneous in thickness (Fig. 4d): from 37 nm immediately at the cross walls up to 92 nm away from the cross walls. The external serrated layer was consistently ca. 50 nm thick. Trichomes were surrounded by fibrous extracellular sheaths (hardly or not discernable in a light microscope) of loose structure and consistent density; no layers different in density or structure were observed (Fig. 4a, b). The round oil-like inclusions at cross-walls, which were visible in light microscope, appeared black (image not shown) and showed internal structure. No other types of inclusions were observed.

Autumn Samples

As in the spring samples, the cells contained unfolded nucleoids and polyhedral bodies in the central cytoplasm (Fig. 4e, f). The thylakoid system was well developed: numerous thylakoids were arranged mostly in parallel to the cell walls in the cross sections and often interconnected with each other (Fig. 4f). In the longitude sections, thylakoids formed irregular patterns, or groups of thylakoids were oriented either parallel or perpendicular to the cross walls (Fig. 4e). The thylakoid membranes had very narrow intramembrane space and carried no discernable phycobilisomes viewed with 100,000x magnification. No additional layers associated with the cell walls were observed; neither was the cells surrounded with any extra envelope-like structures (Fig. 4g). The thickness and structure of the cell walls as well as the character of cell division were very similar to those in the early summer. The

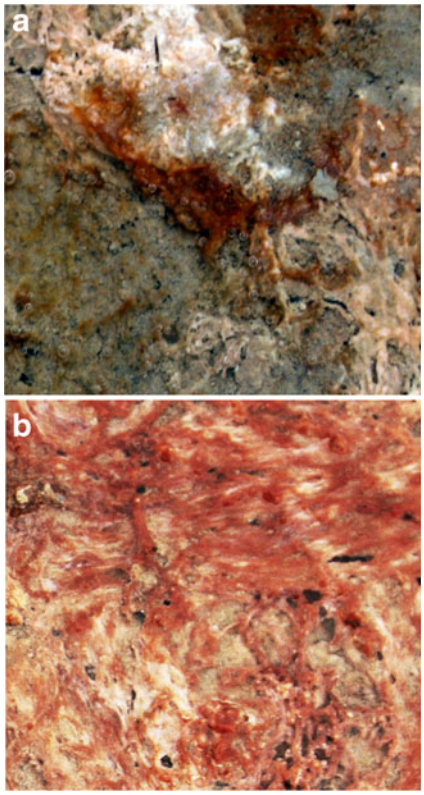

Fig. 5 Fragments of the pool *Phormidium* community in the early summer (**a**) and in autumn (**b**)

trichomes were surrounded with thick fibrous multilayered sheaths. The layers of the sheaths clearly differed in density, which was visible as an alternation of darker and lighter bands (Fig. 4e, f). Only the oil-like inclusions were observed, which appeared similar to those in the spring samples.

Winter Samples

The thylakoid system was very poorly developed: the thylakoids were small and flat and carried no discernable phycobilisomes (Fig. 4h, i). The cell walls appeared similar as in the early summer and autumn cells (Fig. 4j). The other ultrastuctural features did not differ from those in the autumn samples.

Viability and Metabolic Activity During Vegetative Season

Early Summer Samples

Staining with CTC showed that in July, more than 99 % of cells were active (i.e., maintained respiration) in both communities, including filaments from pink biomass, as they reduced CTC to insoluble CTC–formazan crystals. The pattern of CTC deposition in cells (Fig. 2b, g) was similar to that of actively growing laboratory cultures, which we observed in previous experiments [20]. A few inactive cells (CTC negative) were also SYTOX Green positive, indicating damage to their plasma membranes, and therefore were classified as dead cells. A few CTC- and SYTOX-positive cells (i.e., injured) occurred at the polar ends of filaments, whose membranes were apparently damaged due to a disruption of filaments during the staining procedure (Fig. 2a–c). Dormant cells (inactive and intact) were not observed. DAPI staining showed that all nucleoid-containing cells had unfolded nucleoids (Fig. 2d). The content of phycobiliproteins (C-phycoerythrin and C-phycocyanin) seemed to be low as only dim fluorescence was observed under 565–585-nm light (Fig. 2e), which is suitable to excite both pigments [20].

Autumn Samples

In September, as winter approached, the number of injured and dead cells was still very low (<1 %), and nucleoids in live cells remained unfolded (Fig. 6g). All SYTOX Green-negative cells (Fig. 6d) produced CTC–formazan crystals (Fig. 6e), but their size, number, and shape often differed from filament to filament (Fig. 6c). The average number of CTC–formazan deposits per cell seemed to be lower than in spring. Cells in some of the filaments contained only a few deposits, but we did not observe any SYTOX Green-negative cells, which completely lacked deposits (i.e., dormant cells). The fluorescence of phycobiliproteins was more intensive than in the early summer (Fig. 6h).

Winter Samples and Simulation of Spring Thaw

In April, the communities were frozen solid under 35 cm of ice, which was covered with a thin layer of snow. After melting under laboratory conditions, the crusts from samples looked similar to those in September, with pink and red patches of biomass. The filaments had pale-red pigmentation under transmitted light (not shown) and were enclosed in sheaths (Fig. 7b); some of the sheaths were sealed and incrusted with sand at the polar ends (Fig. 7a). Most of the trichomes within sheaths were split into short fragments (hormogonia), whose length varied from one cell to several dozens of cells. Hormogonia were separated from each other with characteristic necridic (dead) cells or by rows of dead cells, which were revealed by simultaneous staining with SYTOX Green, CTC (Fig. 7b–d), and DAPI (not shown). Nucleoids were not condensed and appeared similar as in cells collected during vegetative season (not shown). Apart from necridic cells, live and non-decayed dead cells were morphologically similar (Fig. 7b) and did not notably differ from cells in late summer–autumn period (compare Figs. 3a and 6a). Filaments enclosed in sheaths contained ca. 15 % of dead cells (including necridic cells), whereas sheathless filaments contained as much as 67 % of dead cells. The proportion of dead cells among the sheathless filaments possibly was even higher

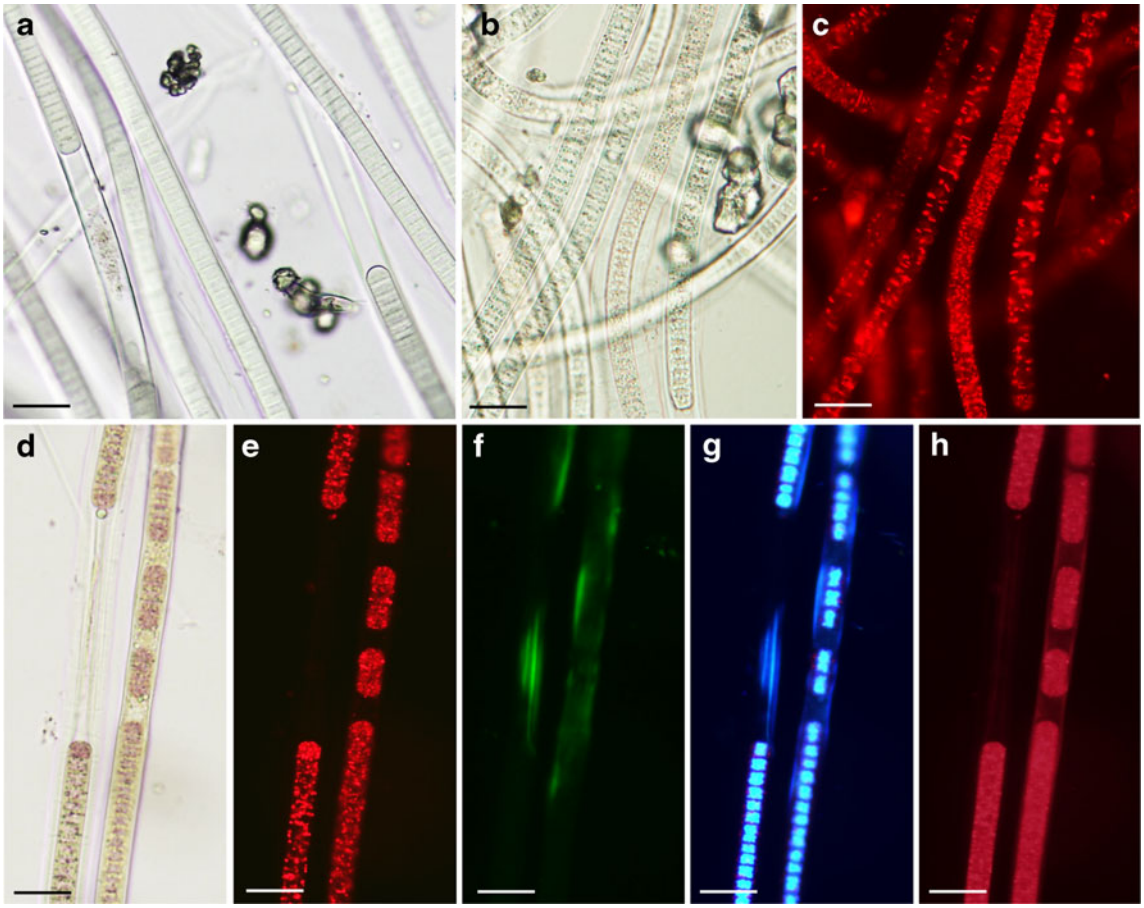

Fig. 6 Filaments from the red areas of the stream community in August (**a**) and second half of September (**b**–**h**), viewed by light microscopy (**a**, **b**, **d**) and stained with CTC (**c**, **e**), SYTOX Green (**f**), and DAPI (**g**) and showing pigment autofluorescence (**h**). Morphologically similar filaments (**b**) display notably different patterns of CTC–formazan deposition (**c**). **a**–**c** Biomass is fixed with formaldehyde. *Scale bars* are 20 μm

because some of the trichomes, containing live cells, might have left their sheaths during melting and staining procedure. Staining the biomass only with CTC immediately after thawing showed that the cells quickly regained respiration activity: just 20 min after melting cells accumulated visible fluorescent inclusions of CTC–formazan. Similar to September, the pattern of CTC deposits within the cells was different in some proportion of filaments and did not correspond with SYTOX Green staining.

During further incubation at low temperature, the morphology of communities and filaments changed markedly. After a day of cultivation, live cells of hormogonia within sheaths turned from pale-red to pale-green, and dead cells sustained lysis and decay (Fig. 8a). During the second day, live cells turned intensively green and moved within the sheaths (Fig. 8b), and the dead cells underwent complete decay. Hormogonia started to escape from the sheaths by gliding out through the polar ends (Fig. 8d), as well as by actively cracking (Fig. 8c) and dissolving the sheaths (Fig. 8e) wherever the polar ends of the sheaths were blocked. After 7 days of cultivation, a substantial number of trichomes were out of the sheaths, and after 15 days, some of the trichomes started to accumulate at cross walls similar material as those in the samples collected in the early summer (data not shown).

Discussion

Viability, Metabolic Activity, and Morphology of Cells

The microalgae, which inhabit terrestrial and hydro-terrestrial environments in the Polar Regions, form annual or perennial communities [5, 27, 28]. The annual growth implies that the communities are re-established every year from a few highly resistant cells while the majority of cells do not survive winter; this strategy is rather common for eukaryotic microorganisms, e.g., green algae [17, 28, personal observation]. In contrast, cyanobacteria typically form perennial mats and films, in which a large proportion of cells survive winter to provide high inoculum for the following vegetative season. Slow biomass accumulation on new substrates and very low photosynthetic rates suggest that extremely high biomass of

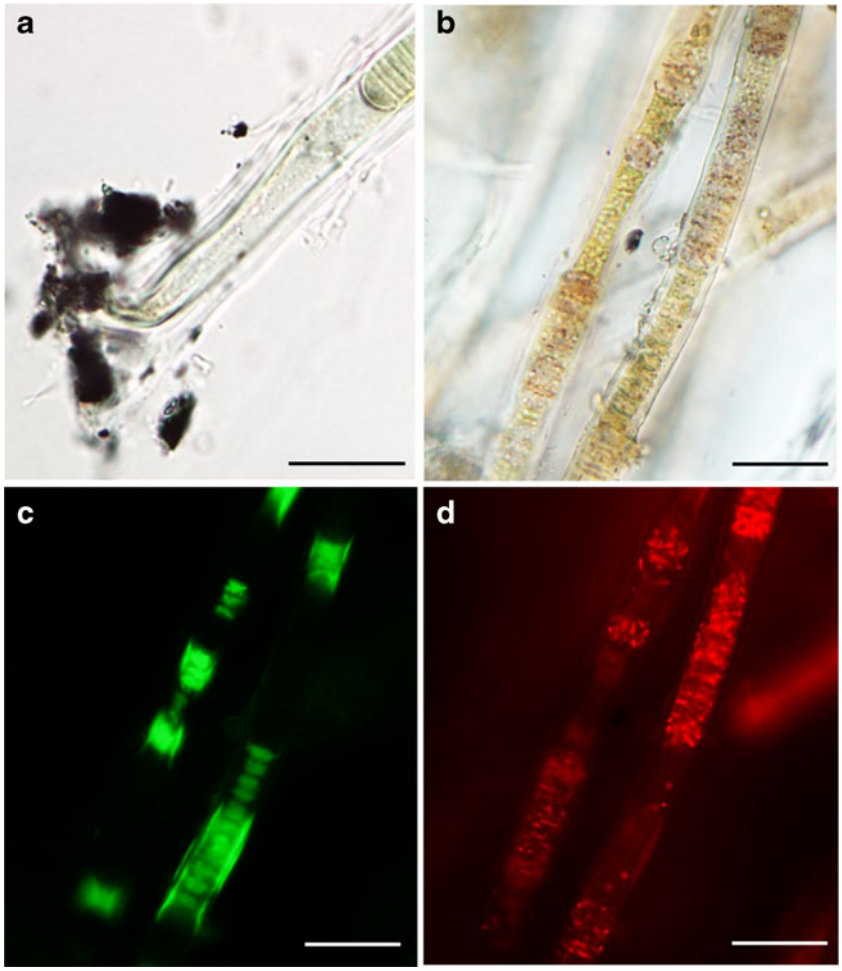

Fig. 7 Morphology and viability of cells and filaments after melting, viewed by light microscopy (**a**, **b**) and stained with SYTOX Green (**c**) and CTC (**d**); dead cells are SYTOX Green positive and CTC negative. *Scale bars* are 20 μm

Phormidium mats can be achieved only over several seasons of growth [5, 18]. The ability of *Phormidium* species to tolerate desiccation and freezing provides additional evidence of their perennial life strategy [19, 29]. In these studies, perennial strategy of *Phormidium* communities was described using community-level-based methods such as measurements of respiratory and photosynthetic rates. However, no study previously described the changes in spatial structure of communities, morphology and ultrastructure of cells, and viability and activity at the single-cell level.

In this study, we demonstrate that the *Phormidium* communities did not produce any morphologically and/or ultrastructurally distinct spore-like cells at the end of the vegetative season for surviving the winter period, unlike akinete-forming cyanobacteria [30] and some species of non-akinete-forming cyanobacteria [31]. The winter survival of the communities was also not provided by a few resistant cells, which did not undergo visible morphological and ultrastructural transformations. Instead, a high proportion of cells from the frozen samples remained viable, indicating that most of the cells in the populations acquired resistance to winter stress. Such successful overwintering provides additional evidence that *Phormidium* species form perennial communities in hydro-terrestrial habitats of Polar Regions. The proportion of cells that survive winter may be normally even higher than 85 %. In our observations, the survival rate was possibly lowered by the 2-week thawing period during winter when no light was available for photosynthesis, and the cells could have been de-hardened by the presence of low-salinity liquid water.

We have shown that all live cells in the communities were constantly metabolically active from early spring to late autumn and overwintered in a vegetative state since they resumed respiration within minutes after thawing. Using community-level methods, several studies have previously demonstrated that respiration in *Phormidium*-dominated mats could be detected immediately after thawing and rehydration [5, 19]. However, this could have been attributed to the other organisms highly abundant in mixed mat communities, such as heterotrophic bacteria, protists, and invertebrates. Here, we demonstrated that cyanobacterial cells themselves were capable of resuming respiration after prolonged freezing. In addition, nucleoids remained unfolded at any time of observations, which indicated that cells did not have long-term cessation of

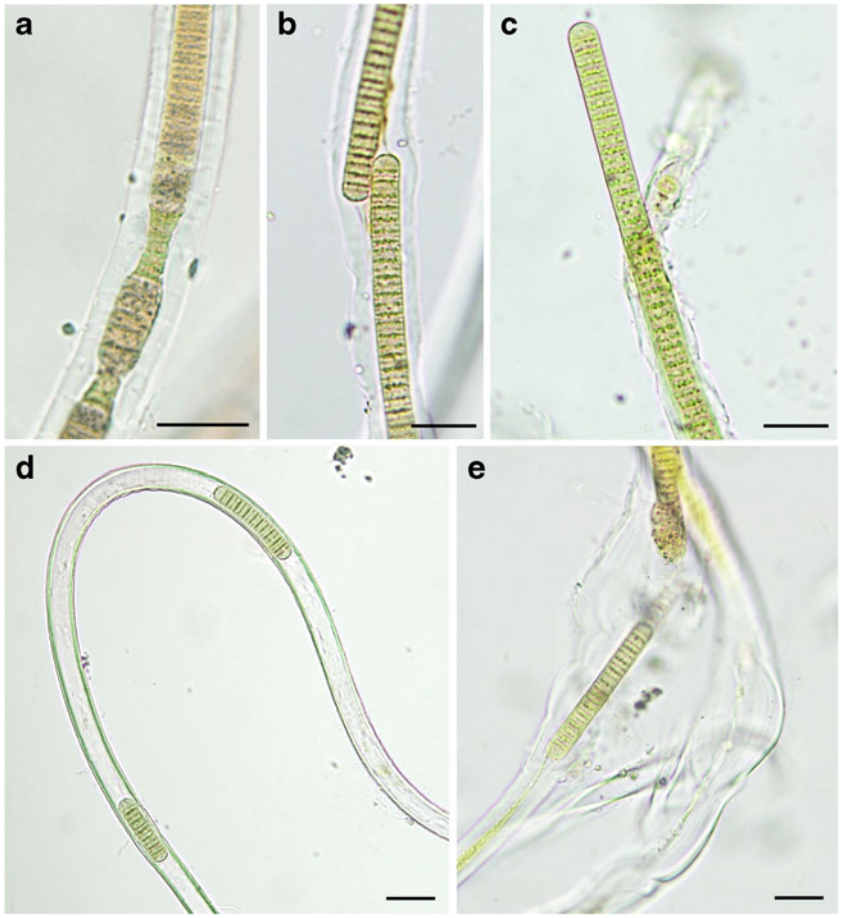

Fig. 8 Morphology of filaments during the first week after melting. Dead cell decay (**a**) and hormogonia (short fragments of trichomes) move inside firm EPS sheaths (**b**) and are released from their sheaths through the ends (**d**) or by cracking (**c**) and dissolving sheaths (**e**). *Scale bars* are 20 μm

transcription activity, which accompanies transition of cells into a dormant state. In metabolically inactive cells, the nucleoids are typically condensed and attain a spherical or toroid shape [32, 33].

Taken together, it seems that communities were inactive only when they were limited by an absence of liquid water during the winter months and possibly during seasonal dry up. In addition to the short vegetative seasons on Svalbard, which in our data were 3.5 to 4 months, very shallow aquatic habitats there are subject to drying–rewetting and freeze–melting cycles. The fact that communities do not need to enter dormancy (and to carry subsequent germination) for surviving stress conditions seems to give an advantage to slow-growing cyanobacteria. This strategy prolongs the growth period and enables them to continue their growth immediately after conditions become favorable.

Adaptation to Winter Abiotic Stress

The main stresses associated with freezing are cell dehydration and mechanical disruption of cell structures by ice crystals [2, 34, 35]. Dehydration occurs as a result of freezing external (i.e., extracellular) medium. As water freezes, osmotic pressure in unfrozen water around ice crystals increases due to a concentration of solutes. As a result, water outflows from cells along the osmotic gradient and freezes in extracellular media, and the residual intracellular water does not freeze even at low subzero temperatures. Freeze-induced dehydration prevents intracellular freezing, which is usually fatal for cells. Expanding extracellular ice creates mechanical pressure on cells, and growing ice crystals may pierce cell plasma membranes [34].

It is not likely that freezing is initiated at the surface of cells because cyanobacterial cells themselves are relatively poor ice nucleators, e.g., lichen photobionts [36]. Our previous (unpublished) experiments showed that laboratory-grown *Phormidium*/*Microcoleus* cultures, isolated from terrestrial habitats of the Arctic and Antarctic, initiated freezing at temperatures as low as −10 to −8 °C (measured with differential scanning calorimetry) after rinsing them with ultrapure water. More probably, freezing takes place at higher subzero temperatures (i.e., close to 0 °C) in water that surrounds communities because water normally contains bacteria as well as various organic and inorganic particles that serve as ice nucleators [37, 38]. In this case, EPS sheaths may function as a barrier that protects surface of cells from being in direct contact with ice crystals. The fact that a much smaller percentage of cells among sheathless trichomes survived freezing supports this

assumption. Apart from sheath production and light-dependent modification of thylakoids, the cells and filaments from winter samples were similar in morphology and ultrastructure to those in late spring. Therefore, it is likely that cells acquire tolerance to freezing-associated dehydration via biochemical mechanisms, e.g., accumulation of non-reducing sugars [39].

Environmental Signals, Which Induce Stress Resistance

Desiccation and freezing tolerance of communities in early summer and in autumn still has to be compared to find out whether their tolerance is an induced or a constitutive property. Nevertheless, we assume that populations change their rate of stress tolerance during the vegetative season: our previous investigations demonstrated that desiccation tolerance of *Microcoleus* from terrestrial Arctic habitats was not a constitutive trait but inducible by suboptimal conditions [40]. We expected that a seasonal decrease of mineral nutrients, especially forms of nitrogen, or even starvation would stimulate cyanobacterial cells to adapt to freezing and desiccation. This assumption was based on the fact that nutrient starvation is a very common inducer of bacterial tolerance to various stresses [41, 42] and that nitrogen concentration in freshwater polar habitats (McMurdo region, Antarctica) may decline by three orders of magnitude over the course of the vegetative season [5]. In addition, our recent experiments showed that *Microcoleus* strains from terrestrial Arctic habitats acquired a strong desiccation tolerance after a 2-week nitrogen starvation [40]. However, a decrease in content of macronutrients was not observed: the communities were constantly well supplied with nitrogen the whole season and constantly limited with dissolved forms of phosphorus.

Continuous light, especially high intensity, nitrogen starvation, and hyperosmotic stress are among the most common inducers of EPS production in cyanobacteria [43]. The climatic data suggest that light regime and its intensity did not play a role in the induction of sheath production, since the duration and intensity of sunlight were decreasing toward the end of the vegetative season. Neither was the production of sheaths dependent on nitrogen availability: concentration and forms of dissolved nitrogen did not significantly change during the vegetative season. The temperature regime during summer did not seem to be the cause either because except for a short period after the snowmelt, the temperature regime was relatively stable until autumn.

Therefore, we hypothesize that increasing the conductivity of water in habitats toward the end of vegetative season stimulated the synthesis of EPS sheaths as well as the acquisition of adaptation to freezing-associated dehydration. The other factors which may influence EPS production, e.g., dilution rate, growth phase, and presence/absence of metal cations and small organic molecules, have been sporadically studied, but not consistently evaluated [43].

The Role of Hormogonia in Dissemination and Spatial Structure of the Communities

Apparently, release of hormogonia in spring resulted in the formation of pale-pink and red areas, which we observed in the field at the beginning of summer: pink areas consisted of mainly empty sheaths remaining after the release of hormogonia, and soft red biomass contained viable and growing sheathless trichomes. Production of new sheaths at the end of the summer was responsible for the appearance of tight continuous crusts with distinctly different pink (mostly empty sheaths) and red (filaments in thick sheaths) parts.

It is thought that hormogonia serve for dispersing cyanobacteria since short sheathless fragments of trichomes may be passively transported by water flow or actively by gliding, as well as for reproduction because a hormogonium consisting of a few cells develops further into a long filament [44, 45]. We observed that during the spring melt, *Phormidium* hormogonia were actively leaving their sheaths, not only through the polar ends, but also by dissolving their sheaths partly or entirely. Partial dissolution of sheaths possibly prevented a massive accumulation of empty sheaths over several years. Interestingly, a proportion of trichomes with metabolically active and intact cells remained in their sheaths for the entire season.

It is not clear whether the production of hormogonia takes place in late autumn shortly before freezing or in early spring when liquid water becomes available. As we observed, only a small proportion of hormogonia was produced at the end of September, but in the winter samples (the first half of April), nearly all trichomes were fragmented immediately after melting. Hormogonia might have been produced during the uncommon-for-winter 2-week period of thaw in January 2012. Hormogonium production may be stimulated by environmental changes both positive and negative for growth and include changes in light, temperature, and chemical composition of an environment [46]. However, no single environmental factor has been identified that induces hormogonium differentiation in all capable strains [44, 45]. In our case, differentiation of hormogonia might have been positively stimulated during the winter thaw by an increase of temperature and dilution of concentrated salt solution surrounding ice crystals with meltwater. The production and release of hormogonia during winter do not seem to have any benefits, because sheathless trichomes are more susceptible to damage imposed by ice crystals (as shown in this study). Therefore, it is more likely that hormogonia are normally produced during spring melt.

Interestingly, viable hormogonia were separated from each other not only by characteristic necridic cells (necessary for fragmentation of trichomes in species with tight cell-to-cell connections), but also by rows of several dead cells. There

was no obvious reason for that phenomenon since all cells inside a sheath had similar environmental conditions. However, we may hypothesize that they lost viability due to self-mediated autolysis in response to environmental cues [47, 48] with a function of nutrient supply of live cells, as some *Phormidium* species are capable of switching to heterotrophic metabolism in the absence of light [49, 50].

Conclusions

The two *Phormidium*-dominated communities were found to be perennial since a high proportion of cells survived winter. The overwintering strategy did not involve any morphological and ultrastructural modifications of cells. However, production of thick polysaccharide sheaths was likely to protect the cells from damage by freezing and freeze-induced dehydration. The cells were metabolically active shortly before freezing and immediately after thawing, which means that communities survived winter in a vegetative state. The communities changed their spatial structure over the annual cycle: release of hormogonia in spring resulted in the formation of a subpopulation of sheathless trichomes along with a tight crust which was composed mostly of empty polysaccharide sheaths and a few viable trichomes. The length of the active period of growth (or vegetative season) over the annual cycle was defined by the presence of water in the liquid state; i.e., the metabolic activity of cyanobacteria was discontinued only by freezing in winter. The cells did not change their morphology and ultrastructure during the vegetative season, except for light-induced modification of thylakoids.

Acknowledgments This research was supported by projects from the Ministry of Education of the Czech Republic (KONTAKT ME 934, INGO LA 341, and LM2010009 CzechPolar), by project reg. no. CZ.1.07/2.2.00/28.0190 funded by the European Social Fund and from the government budget of the Czech Republic, and as a long-term research development project of the Academy of Sciences of the Czech Republic RVO 67985939. We thank Dr. Lenka Bučinská for assistance with electron microscopy, Drs. Anne Jungblut, Jiří Komárek, Linda Nedbalová and Warwick Vincent for helpful discussions, and the anonymous reviewers for improving the manuscript.

References

1. Quesada A, Vincent WF (2012) Cyanobacteria in the cryosphere: snow, ice and extreme cold. In: Ecol. Cyanobacteria II. Springer Netherlands, Dordrecht, pp 387–399
2. Tashyreva D, Elster J (2012) Production of dormant stages and stress resistance of polar Cyanobacteria. In: Hanslmeier A, Kempe S, Seckbach J (eds) Life earth other planet. Bodies, pp 367–386
3. Vincent W (2002) Cyanobacterial dominance in the Polar Regions. In: Whitton B, Potts M (eds) Ecol. Cyanobacteria SE - 12. Springer Netherlands, pp 321–340
4. Elster J (2002) Ecological classification of terrestrial algal communities in polar environments. Geoecology Antarctic ice-free coastal landscapes. Ecol Stud 154:303–326
5. Vincent W, Howard-Williams C (1986) Antarctic stream ecosystems: physiological ecology of a blue-green algal epilithon. Freshw Biol 16:219–233. doi:10.1111/j.1365-2427.1986.tb00966.x
6. Block W, Lewis Smith RI, Kennedy AD (2009) Strategies of survival and resource exploitation in the Antarctic fellfield ecosystem. Biol Rev 84:449–484. doi:10.1111/j.1469-185X.2009.00084.x
7. Fritsen CH, Priscu JC (1998) Cyanobacterial assemblages in permanent ice covers on Antarctic lakes: distribution, growth rate, and temperature response of photosynthesis. J Phycol 34:587–597. doi:10.1046/j.1529-8817.1998.340587.x
8. McKnight DM, Howes BL, Taylor CD, Goehringer DD (2000) Phytoplankton dynamics in a stably stratified winter lakes during winter darkness. J Phycol 36:852–861
9. Vincent WF, Quesada A (2012) Cyanobacteria in high latitude lakes, rivers and seas. In: Whitton BA (ed) Ecol. Cyanobacteria II. Dordrecht, Springer Netherlands, pp 371–385
10. Láska K, Witoszová D, Prošek P (2012) Weather patterns of the coastal zone of Petuniabukta, central Spitsbergen in the period 2008–2010. Polish Polar Res 33:297–318. doi:10.2478/v10183-012-0025-0
11. Davey M (1989) The effects of freezing and desiccation on photosynthesis and survival of terrestrial Antarctic algae and cyanobacteria. Polar Biol 29–36
12. Howard-Williams C, Vincent WF (1989) Microbial communities in southern Victoria Land streams (Antarctica) I. Photosynthesis. Hydrobiologia 172:27–38. doi:10.1007/BF00031610
13. Jungblut A-D, Hawes I, Mountfort D et al (2005) Diversity within cyanobacterial mat communities in variable salinity meltwater ponds of McMurdo Ice Shelf, Antarctica. Environ Microbiol 7: 519–529. doi:10.1111/j.1462-2920.2005.00717.x
14. Toro M, Camacho A, Rochera C et al (2007) Limnological characteristics of the freshwater ecosystems of Byers Peninsula, Livingston Island, in maritime Antarctica. Polar Biol 30:635–649. doi:10.1007/s00300-006-0223-5
15. Komárek J, Elster J, Komárek O (2008) Diversity of the cyanobacterial microflora of the northern part of James Ross Island, NW Weddell Sea, Antarctica. Polar Biol 31:853–865. doi:10.1007/s00300-008-0424-1
16. Komárek J, Kováčik L, Elster J, Komárek O (2012) Cyanobacterial diversity of Petuniabukta, Billefjorden, central Spitsbergen. Polish Polar Res. doi:10.2478/v10183-012-0024-1
17. Davey MC (1991) Effects of physical factors on the survival and growth of Antarctic terrestrial algae. Br Phycol J 26:315–325. doi:10.1080/00071619100650281
18. Hawes I, Howard-Williams C (2013) Primary production processes in streams of the Mcmurdo Dry Valleys, Antarctica, pp 129–140
19. Hawes I, Howard-Williams C, Vincent W (1992) Desiccation and recovery of Antarctic cyanobacterial mats. Polar Biol 587–594.
20. Tashyreva D, Elster J, Billi D (2013) A novel staining protocol for multiparameter assessment of cell heterogeneity in *Phormidium* populations (Cyanobacteria) employing fluorescent dyes. PLoS One 8, e55283. doi:10.1371/journal.pone.0055283
21. Komárek J, Anagnostidis K (2005) Süßwasserflora von Mitteleuropa, Bd. 19/2: Cyanoprokaryota, 1st ed. Springer Spektrum
22. Casamatta DA, Johansen JR, Vis ML, Broadwater ST (2005) Molecular and morphological characterization of ten polar and near-polar strains within the Oscillatoriales (Cyanobacteria). J Phycol 41:421–438. doi:10.1111/j.1529-8817.2005.04062.x
23. Strunecký O, Komárek J, Johansen J et al (2013) Molecular and morphological criteria for revision of the genus *Microcoleus*

(Oscillatoriales, Cyanobacteria). J Phycol 49:1167–1180. doi:10.1111/jpy.12128
24. Sciuto K, Andreoli C, Rascio N et al (2012) Polyphasic approach and typification of selected *Phormidium* strains (Cyanobacteria). Cladistics 28:357–374
25. Komárek J, Kastovsky J, Mares J, Johansen JR (2014) Taxonomic classification of cyanoprokaryotes (cyanobacterial genera) 2014, using a polyphasic approach. Preslia 295–335.
26. Hoiczyk E, Hansel A (2000) Cyanobacterial cell walls: news from an unusual prokaryotic envelope. J Bacteriol 182:1191–1199. doi:10.1128/JB.182.5.1191-1199.2000
27. Hawes I (1989) Filamentous green algae in freshwater streams on Signy Island, Antarctica. Hydrobiologia 172:1–18. doi:10.1007/BF00031608
28. Hawes I (1990) Effects of freezing and thawing on a species of *Zygnema* (Chlorophyta) from the Antarctic. Phycologia 29:326–331. doi:10.2216/i0031-8884-29-3-326.1
29. Šabacká M, Elster J (2006) Response of cyanobacteria and algae from Antarctic wetland habitats to freezing and desiccation stress. Polar Biol 30:31–37. doi:10.1007/s00300-006-0156-z
30. Mehnert G, Rucker J, Wiedner C (2014) Population dynamics and akinete formation of an invasive and a native cyanobacterium in temperate lakes. J Plankton Res 36:378–387. doi:10.1093/plankt/fbt122
31. Billi D, Caiola MG (1996) Effects of nitrogen limitation and starvation on *Chroococcidiopsis* sp. (Chroococcales). New Phytol 133:563–571. doi:10.1111/j.1469-8137.1996.tb01925.x
32. Robinow C, Kellenberger E (1994) The bacterial nucleoid revisited. Microbiol Rev 58:211–232
33. Frenkiel-Krispin D, Ben-Avraham I, Englander J et al (2004) Nucleoid restructuring in stationary-state bacteria. Mol Microbiol 51:395–405. doi:10.1046/j.1365-2958.2003.03855.x
34. Mazur P (1984) Freezing of living cells: mechanisms and implications. Am J Physiol 247:C125–C142
35. Thomashow MF (1998) Role of cold-responsive genes in plant freezing tolerance. Plant Physiol 118:1–7. doi:10.1104/pp.118.1.1
36. Kieft TL, Ahmadjian V (1989) Biological Ice nucleation activity in lichen mycobionts and photobionts. Lichenol 21:355. doi:10.1017/S0024282989000599
37. Lundheim R (2002) Physiological and ecological significance of biological ice nucleators. Philos Trans R Soc Lond B Biol Sci 357:937–943. doi:10.1098/rstb.2002.1082
38. Christner BC, Cai R, Morris CE et al (2008) Geographic, seasonal, and precipitation chemistry influence on the abundance and activity of biological ice nucleators in rain and snow. Proc Natl Acad Sci 105:18854–18859. doi:10.1073/pnas.0809816105
39. Hershkovitz N, Oren A, Cohen Y (1991) Accumulation of trehalose and sucrose in cyanobacteria exposed to matric water stress. Appl Environ Microbiol 57:645–648
40. Tashyreva D, Elster J (2015) Effect of nitrogen starvation on desiccation tolerance of Arctic *Microcoleus* strains (cyanobacteria). Front Microbiol 6:1–11. doi:10.3389/fmicb.2015.00278
41. McCann MP, Kidwell JP, Matin A (1991) The putative sigma factor KatF has a central role in development of starvation-mediated general resistance in *Escherichia coli*. J Bacteriol 173:4188–4194. doi:10.1016/0378-1097(92)90039-Q
42. Siegele DA, Kolter R (1992) Life after log. J Bacteriol 174:345–348
43. Pereira S, Zille A, Micheletti E et al (2009) Complexity of cyanobacterial exopolysaccharides: composition, structures, inducing factors and putative genes involved in their biosynthesis and assembly. FEMS Microbiol Rev 33:917–941. doi:10.1111/j.1574-6976.2009.00183.x
44. Meeks JC, Elhai J (2002) Regulation of cellular differentiation in filamentous cyanobacteria in free-living and plant-associated symbiotic growth states. Microbiol Mol Biol Rev 66:94–121. doi:10.1128/MMBR.66.1.94
45. Flores E, Herrero A (2010) Compartmentalized function through cell differentiation in filamentous cyanobacteria. Nat Rev Microbiol 8:39–50. doi:10.1038/nrmicro2242
46. Marsac NT, Govindjee, Amesz J et al. (2004) Differentiation of hormogonia and relationships with other biological processes. In: Mol. Biol. Cyanobacteria, pp 825–842
47. Franklin DJ, Brussaard CPD, Berges JA (2006) What is the role and nature of programmed cell death in phytoplankton ecology? Eur J Phycol 41:1–14. doi:10.1080/09670260500505433
48. Navarro Llorens JM, Tormo A, Martínez-García E (2010) Stationary phase in gram-negative bacteria. FEMS Microbiol Rev 34:476–495. doi:10.1111/j.1574-6976.2010.00213.x
49. Pope D (1974) Heterotrophic potential of *Phormidium* and other blue-green algae. Can J Bot 52:2369–2374
50. Khoja TM, Whitton BA (1975) Heterotrophic growth of filamentous blue-green algae. Br Phycol J 10:139–148. doi:10.1080/00071617500650131